

Self-organization of internal pedestals in a sandpile

This content has been downloaded from IOPscience. Please scroll down to see the full text.

2003 Plasma Phys. Control. Fusion 45 301

(<http://iopscience.iop.org/0741-3335/45/3/310>)

View [the table of contents for this issue](#), or go to the [journal homepage](#) for more

Download details:

IP Address: 137.205.62.4

This content was downloaded on 22/01/2014 at 19:47

Please note that [terms and conditions apply](#).

Self-organization of internal pedestals in a sandpile

S C Chapman¹, R O Dendy^{2,1} and B Hnat¹

¹ Space and Astrophysics Group, Department of Physics, Warwick University,
Coventry CV4 7AL, UK

² EURATOM/UKAEA Fusion Association, Culham Science Centre, Abingdon,
Oxfordshire OX14 3DB, UK

Received 13 November 2002

Published 24 February 2003

Online at stacks.iop.org/PPCF/45/301

Abstract

The temperature profiles of magnetically confined plasmas can display distinctive longlived internal pedestals, caused by self-created transport barriers. This raises theoretical physics issues, distinct from the plasma physics modelling challenge, which concern the class of transport processes, physical principles, and control parameters that can generate such phenomenology. Here, we show that such structures can arise naturally through avalanching transport in a sandpile model. A single control parameter, that governs the spatial range of each rapid critical-gradient-triggered redistribution event, determines the occurrence and regularity of these effects.

1. Introduction

A distinctive feature of magnetically confined plasmas is that they can sustain local regions having very steep (indeed, almost discontinuous) temperature gradients. Pedestals in the edge temperature are a key feature of the H-mode good confinement regimes of tokamaks (for a recent review see, e.g. [1]). Additionally, advanced operating regimes for tokamaks have now been accessed, which involve the creation of internal transport barriers (ITBs)—persistent steplike features in the temperature profiles internal to the plasma (see, e.g. [2–6]). In some cases, multiple barriers are seen. The occurrence of such structures in externally heated plasma systems that are diffuse, high temperature, and turbulent is surprising, and is a striking instance of their capacity for macroscopic self-organization. It raises theoretical physics issues that are distinct from the important challenge of modelling these structures using the techniques of plasma physics. For example, one may ask: what classes of transport process are compatible with barrier formation and persistence, what minimal set of governing physical principles can generate internal barriers to transport in macroscopic systems, and how many underlying control parameters need there be? In this paper, we identify how internal barriers to transport can arise spontaneously in the sandpile model of Chapman [7]. Because of the simplicity of this model, it is possible to formally characterize and explain the mechanisms underlying internal pedestal formation, and to identify possible links to aspects of tokamak plasma behaviour. This approach is intended to be complementary to studies that

employ largescale numerical simulation of tokamak plasmas, which have had some success in illuminating the subtle interplay between turbulence and bulk flows that may give rise to ITBs [6, 8]. This paper builds on the results of Chapman *et al* [9], where it was shown that the sandpile model of Chapman [7] can generate edge pedestals, enhanced confinement, and avalanches involving mass loss that share key characteristics with edge localized modes (ELMs) in tokamaks.

2. The sandpile model

The essential ingredients of the N cell sandpile algorithm of Chapman [7] are: (i) critical gradients z_c which must be exceeded locally before any transport can take place, and whose values are randomly re-assigned after each avalanche; (ii) central fuelling at cell $j = 1$, so that sand can only leave the system from the $j = N$ cell by means of systemwide avalanches; and (iii) its only distinctive feature, namely a characteristic lengthscale L_f for fast redistribution which may be considered a proxy for turbulent transport, as discussed in [9]. Where the critical gradient z_c is exceeded at the j th cell the sandpile is flattened behind this unstable cell over a ‘fluidization length’ L_f , embracing the cells $j - (L_f - 1), j - (L_f - 2), \dots, j$; and this sand is conservatively relocated to the cell at $j + 1$. The mean value of z_c is taken to be independent of position across the sandpile. The timestep follows from the inverse inflow rate of sand, which must be multiplied by the product of the average critical gradient and the cell size [10].

Evidence for avalanche-type transport from tokamak experiments [11, 12] and numerical simulations [13, 14] provides growing support for the applicability in some circumstances of the sandpile paradigm introduced into fusion plasma physics in recent years [15–19]. Particularly relevant to this paper are observations and analysis [20, 21] of edge plasma turbulence in a range of magnetically confined plasmas. These suggest that edge plasma turbulence—the environment in which H-mode edge pedestals form, which then coexist with the turbulence—self-organizes into a state that is independent of the size and plasma characteristics of the devices considered. It is known [9] that, depending on the value of the control parameter L_f , the statistical behaviour of the sandpile model of Chapman [7] displays features reminiscent of enhanced confinement phenomenology in tokamaks. These include the time averaged height profiles, which possess edge pedestals in the good confinement regime; furthermore the frequency of systemwide avalanches resulting in mass loss depends on stored sandpile energy in a similar way to that in which the frequency of ELMs depends on stored energy in some tokamak plasmas (see figure 6 of Chapman *et al* [9]). Empirically, good confinement is found [9] to arise when $L_f/N < \frac{1}{4}$. We emphasise that L_f is kept constant across the sandpile in any given computational run, so that the critical gradient and redistribution rules are identical at every cell of our sandpile, apart from the initial and final cells. It follows that where pedestals arise, they represent a true emergent phenomenon. In this respect our approach differs essentially from that of Newman *et al* [15] and Hicks and Carreras [19], where a local transport barrier is implicit at the outset, insofar as the critical gradient and redistribution rules are specified to be different for a particular local group of cells.

3. Self-organization of internal barriers to transport

The three-dimensional plot of figure 1 shows sandpile height as a function of position as time evolves, with $L_f = 50$ in a 512 cell system. It displays two distinct phases. First, there is a relaxation phase where the sandpile profile is smooth down to the self-organized edge pedestal, except within a distance L_f of the core where fuelling has a continual local effect.

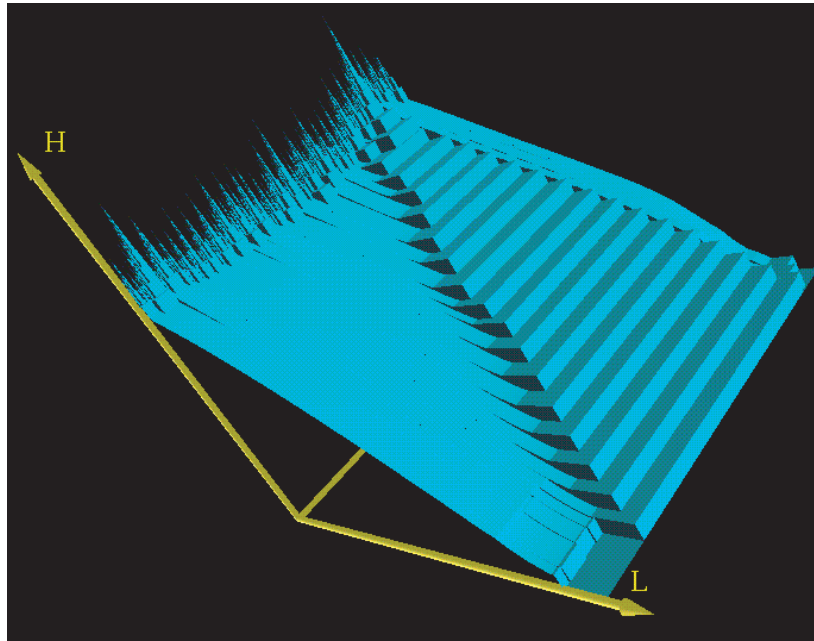


Figure 1. Three-dimensional view of the sandpile height profile for $L_f = 50$. Time evolves along the partially hidden axis. From left to right (increasing time) the plot shows the end of a relaxation phase, a growth phase and the beginning of a second relaxation phase. Plots of local gradient for five such cycles are shown in figure 3(a).

During the relaxation phase mass loss occurs via many systemwide avalanches closely spaced in time, which carry sand over the sandpile boundary. The relaxation phase terminates with a final systemwide avalanche, after which the growth phase begins. The growth phase is characterized by a stationary edge pedestal which resides at the outermost cell of the sandpile. As time progresses, additional pedestals (localized regions of steep gradient just below critical) form successively at positions increasingly close to the core of the sandpile, with average separation $\sim L_f$. Each of these is generated at positions where (outward propagating) major internal avalanches have come to rest. Runs for all values of L_f show that the separation between internal pedestals is not linearly proportional to L_f . Like many ITBs observed in tokamaks, the internal barriers to transport in the sandpile can persist once they have formed, depending as we shall see on the value of L_f . In the example of figure 1 they are terminated only by an event which is unrelated to the transport and the profile, namely the filling up of the sandpile to its maximum extent followed by a systemwide avalanche.

Figure 2 is motivated by simultaneous multichannel measurements of tokamak temperature profiles in the presence of ITBs (see, e.g. figure 3 of Burrell *et al* [3] and figure 1 of Kinsey *et al* [6], and also the results of numerical simulations shown in figure 2 of Kinsey *et al* [6]). Figure 2 shows sandpile height at different positions from the edge to the centre. Just over two growth and relaxation phases are shown. The successive formation of internal pedestals is reflected in a stepwise increase in height at any given point during the growth phases. Using this diagnostic, evidence for stepwise increments is clearest in the region of the sandpile that lies neither at the core nor near the edge (e.g. traces (b)–(d)). Since the internal pedestals form at locations increasingly close to the core as the growth phase proceeds, the

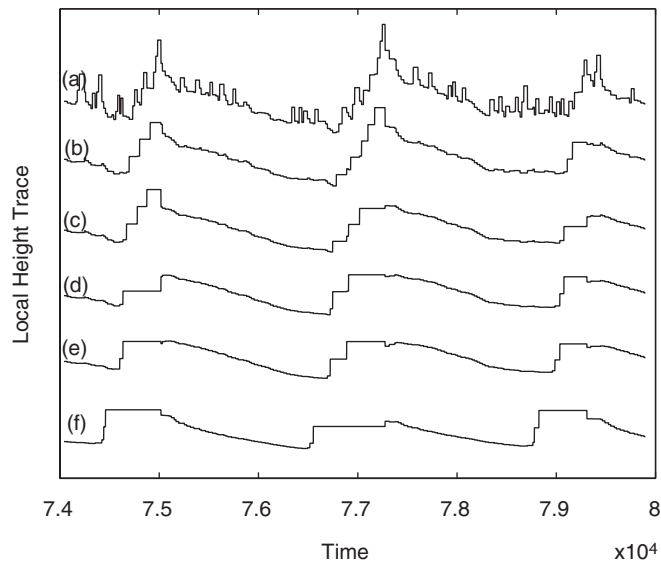


Figure 2. Local height of sand as a function of time at different locations in the sandpile relative to the centre cell $j = 1$: (a) $j = 20$, (b) $j = 65$, (c) $j = 100$, (d) $j = 125$, (e) $j = 150$ and (f) $j = 300$. System size $N = 512$, control parameter $L_f = 50$. The corresponding range of heights explored is: (a) 15.6–22.1, (b) 14.4–19.1, (c) 13.5–17.2, (d) 12.8–15.1, (e) 11.9–14.2 and (f) 6.8–9.1.

points within the sandpile that are most affected by the formation of these pedestals are those that are closer to the core of the sandpile. Points nearer the edge are only affected by the formation of the first few internal pedestals during the early growth phase (e.g. traces (e) and (f)). The results shown in figure 2, which bear some resemblance to the experimental and numerical results of Burrell *et al* [3] and Kinsey *et al* [6], emerge naturally from the dynamics of the sandpile during the growth phase of its good confinement regime. Central to this structure is the unexpected capacity of this sandpile to organize persistent steep pedestals both at the edge and internally.

The role of these internal pedestals and their relationship to the edge pedestal is highlighted in figure 3: here all cells at which the gradient exceeds $z_c/2$ are marked by black points, while all other cells are left blank. The regular quasiperiodic character of figure 3(a) and the irregular character of figure 3(b) identify them, respectively, with the self-organized and self-organized critical (SOC) states that we have identified elsewhere [9]. In figure 3(b) the edge pedestal is well resolved at all times, but its position changes rapidly and irregularly. In contrast to the situation in figure 3(a), there is no well defined time averaged edge position. Figure 3(a) ($L_f = 50$) follows five of the growth and relaxation cycles shown in figure 2. The edge pedestal is visible close to the sandpile boundary in both the relaxation and the growth phases. Its time behaviour is essentially regular and, as we shall see, orders the structure internal to the sandpile. For any $L_f < N/4$, the location of each internal pedestal is fixed during a given growth phase, so that they persist as distinguishable features of the time averaged phenomenology of the sandpile. In contrast, figure 3(b) shows the behaviour for the poor confinement regime with $L_f = 250 > N/4$. This regime corresponds to a SOC state (see [9] and later). Although the sandpile successively fills and empties, it does so in an irregular manner. Pedestals can be seen both at the edge and internal to the sandpile, but the latter are no longer organized in a coherent pattern that persists over time.

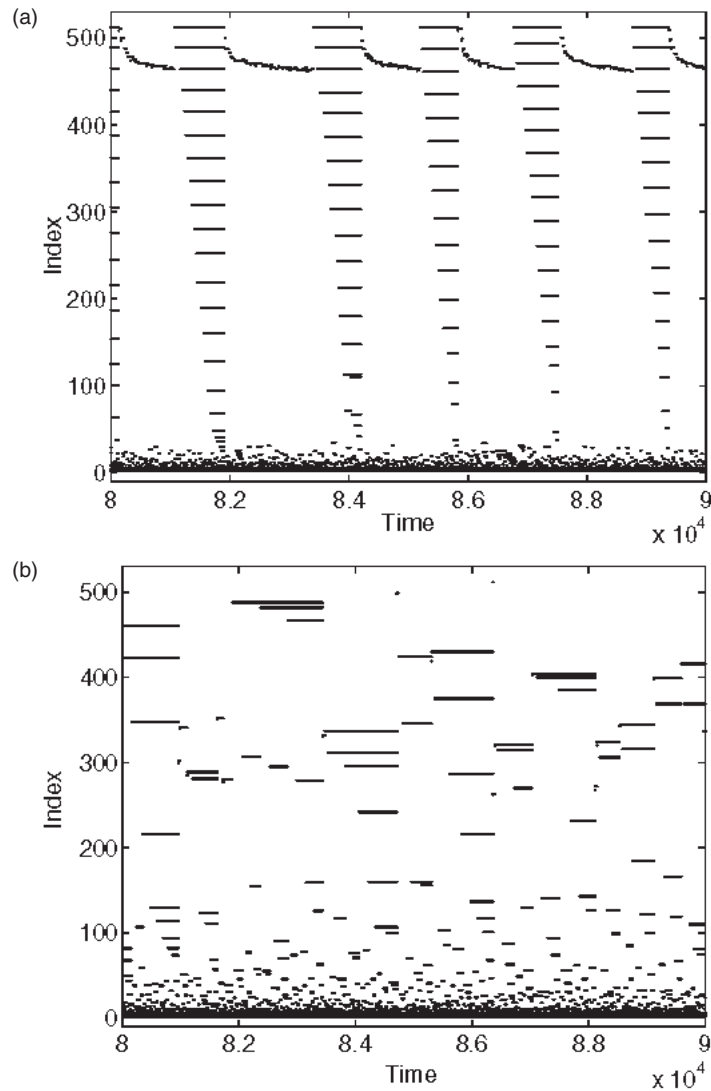


Figure 3. Location of cells where the value of the local gradient exceeds $z_c/2$ for (a) $L_f = 50$ and (b) $L_f = 250$. Zero corresponds to the apex where fuelling occurs. The edge pedestal is visible as the uppermost trace.

A resilient edge pedestal arises for all L_f ; the pedestal is steep, indeed unresolved, in that the entire change in height occurs between neighbouring cells. The location of the edge pedestal is strongly time dependent for large L_f , whereas for small L_f it is confined to a region close to the outermost cell of the sandpile. The time averaged profile in the edge region therefore depends strongly on L_f , and the steadiest edge pedestal corresponds to small L_f and good confinement. Following each avalanche, in our sandpile algorithm the value of the critical gradient z_c is randomized about a mean value at all cells that participated in the avalanche. Nevertheless the gradient at the edge pedestal remains always close to, but just below, the critical value z_c as shown in figure 4. Here the upper traces relate to the outermost occupied cell of the sandpile, where the fluctuating local gradient is seen to remain close to the critical

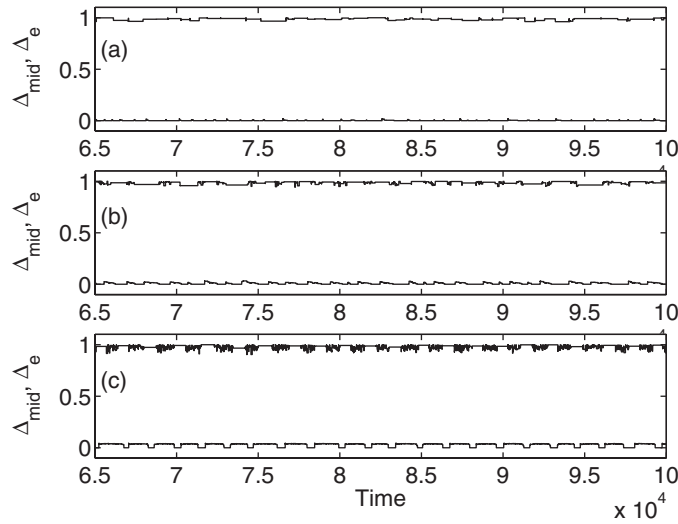


Figure 4. Local gradient normalized to the local value of z_c for the outermost occupied cell (Δ_e , upper traces, value close to unity) and at cell 256 halfway into the sandpile (Δ_{mid} , lower traces, value close to zero), for $L_f = 250$ (a), 150 (b), 50 (c). This shows that the gradient at the edge pedestal always remains close to the critical value throughout. Elsewhere, except where internal pedestals arise (compare figure 3), the local gradient remains well below z_c .

gradient at all times. In contrast, the lower traces show that the fluctuating local gradient near the midpoint of the sandpile remains small compared to the critical gradient. Thus, except where internal or edge pedestals arise, the fluctuating local gradient remains well below the local value of z_c . The internal pedestals appear as barriers to transport: despite their apparent fragility against avalanching (gradient z close to z_c , see figure 3), no sand passes through either the edge or the internal pedestals until the final avalanche that terminates the growth phase.

The physical mechanisms and principles underlying the self-organization of the edge pedestal and multiple internal pedestals that arise in the sandpile model of Chapman *et al* [7, 9] are therefore of considerable interest. As a first step, we confirm the hypothesis of Chapman *et al* [9] that the good confinement regime (small L_f) corresponds to low-dimensional behaviour. From figure 3(a) ($L_f = 50$) we see that the motion of the edge pedestal is quasi-oscillatory and explores a restricted region (from cell 463 to 512). We have also applied the technique of phase space reconstruction by embedding [22] to the time series generated by the edge pedestal position (the last occupied cell in the sandpile). The results show low-dimensional system dynamics that repeatedly follow a simple limit cycle (attractor) around a restricted region of the reconstructed phase space, implying that the large number of cells in the sandpile have self-organized: their collective dynamics are encapsulated by a small number of dynamical variables. Once L_f is increased beyond $L_f = N/4$, this simple quasi-oscillatory behaviour is replaced by stochastic behaviour, consistent with the erratic motion of the edge pedestal seen in figure 3(b); the edge pedestal now also explores a much larger range of the available space (from cell 260 to 512 in this case). Thus increasing complexity of the phase space portrait correlates with deterioration of confinement [9].

For all values of L_f , global relaxation of the sandpile is ultimately achieved by large (systemwide) avalanches. When L_f is of order the system size N , systemwide avalanches are straightforwardly propagated: because $L_f \sim N$, no characteristic scale is imposed by the redistribution process, and the dynamics are self-similar and in SOC (see [23] for a related

treatment of the renormalization group). Conversely, when L_f is significantly distinct from the system size (found empirically to be $L_f < N/4$), there is scale breaking. This leads to broken power law avalanche statistics [7], and the system is no longer in SOC. By separating the characteristic lengthscales we also effectively separate the long term growth-relaxation timescale from the time interval between systemwide avalanches, whereas such a distinction is not possible in the SOC regime. In this good confinement regime (when $L_f < N/4$), the feature evolving on the slow timescale, namely the position of the edge pedestal, effectively determines the details of the internal dynamics. It organizes the sequence of events leading to the successive formation of internal edge pedestals, and the time variation of total energy (sand) in the system. In short, the sandpile is entrained to its edge, and the conditions for self-organization are thereby satisfied. The characteristic signature of the onset of self-organization is low-dimensional dynamics, seen in figures 3(a) and 4 ($L_f = 50$ traces), as opposed to the irregular time evolution and self-similar statistical properties of the system when self-organized and critical (figures 3(b) and 4 ($L_f = 250$ traces)).

4. Conclusions

The confinement physics of our sandpile model offers a robust framework in which a distinctive structure of internal and edge pedestals arises naturally. There is only one control parameter, L_f/N , which governs the spatial range of each rapid critical-gradient-triggered redistribution event and can be considered for example as a proxy for the lengthscale of turbulent transport, normalized to system size. Provided that this lengthscale is sufficiently short, the underlying inverse cascade in real space gives rise to persistent, marginally subcritical profile steps. Furthermore the self-organized edge pedestal is continuously present in all phases of the sandpile evolution, and positions itself exactly at the sandpile boundary throughout the growth phase. These results are sufficient to indicate that some of the distinctive edge and internal pedestal phenomenology seen in tokamak plasmas can also arise in a simpler idealized confinement system, and that they may be linked to the observed avalanching transport phenomena. This suggests that quantitative studies to elucidate the balance between diffusive transport and avalanching transport in tokamaks would be fruitful. The results further suggest a test of the depth of the physical analogy that we have found, as follows. If the analogy is deep, there will exist one or a few dimensionless control parameters, linked to the properties of the turbulent transport, that entirely determine the key features of the confinement phenomenology—regular or irregular—of tokamak plasmas that we have cited here. For example, these parameters would control the extent to which global confinement is entrained to edge pedestal dynamics. The search for such parameters, for example by further application of the techniques of nonlinear time series analysis to edge plasma measurements as initiated in [20, 21], is potentially highly rewarding.

Acknowledgments

We are grateful to George Rowlands and Jack Connor for comments and suggestions. SCC was supported by a PPARC lecturer fellowship, ROD by Euratom and the UK DTI, and BH by HEFCE.

References

- [1] Hugill J 2000 *Plasma Phys. Control. Fusion* **42** R75
- [2] Synakowski E J 1998 *Plasma Phys. Control. Fusion* **40** 581

- [3] Burrell K H *et al* 1998 *Plasma Phys. Control. Fusion* **40** 1585
- [4] de Baar M R *et al* 1999 *Phys. Plasmas* **6** 4645
- [5] Conway G D *et al* 2000 *Phys. Rev. Lett.* **84** 1463
- [6] Kinsey J E, Staebler G M, Burrell K H, Austin M E and Waltz R E 2001 *Phys. Rev. Lett.* **86** 814
- [7] Chapman S C 2000 *Phys. Rev. E* **62** 1905
- [8] Rogers B N, Dorland W and Kotschenreuther M 2000 *Phys. Rev. Lett.* **85** 5336
- [9] Chapman S C, Dendy R O and Hnat B 2001 *Phys. Rev. Lett.* **86** 2814
- [10] Chapman S C, Dendy R O and Rowlands G 1999 *Phys. Plasmas* **6** 4169
- [11] Rhodes T L *et al* 1999 *Phys. Lett. A* **253** 181
- [12] Politzer P A 2000 *Phys. Rev. Lett.* **84** 1192
- [13] Garbet X and Waltz R 1998 *Phys. Plasmas* **5** 2836
- [14] Sarazin Y and Ghendrih P 1998 *Phys. Plasmas* **5** 4214
- [15] Newman D E, Carreras B A, Diamond P H and Hahm T S 1996 *Phys. Plasmas* **3** 1858
- [16] Carreras B A, Newman D, Lynch V E and Diamond P H 1996 *Phys. Plasmas* **3** 2903
- [17] Dendy R O and Helander P 1997 *Plasma Phys. Control. Fusion* **39** 1947
- [18] Chapman S C, Dendy R O and Rowlands G 1999 *Phys. Plasmas* **6** 4169
- [19] Hicks H R and Carreras B A 2001 *Phys. Plasmas* **8** 3277
- [20] Carreras B A *et al* 1998 *Phys. Rev. Lett.* **80** 4438
- [21] Pedrosa M A *et al* 1999 *Phys. Rev. Lett.* **82** 3621
- [22] Ott E 1993 *Chaos in Dynamical Systems* (Cambridge: Cambridge University Press) p 93
- [23] Tam S W Y, Chang T S, Chapman S C and Watkins N W 2000 *Geophys. Res. Lett.* **27** 1367